

Supporting Information

Using Gradient Magnetic Fields to Control the Size and Uniformity of Iron Oxide Nanoparticles for Magnetic Resonance Imaging

Kun Ma^{1#}, Ze Wang^{1, 2#}, Tongxiang Tao^{1, 2#}, Shuai Xu^{1, 2}, Sajid ur Rehman¹, Xu Yan⁴, Jun Fang¹, Ruiguo Chen¹, Hui Wang¹, Xin Zhang¹, Can Xie¹, Yang Lu^{4}, Qingyou Lu^{1, 2*}, Junfeng Wang^{1, 2, 3*}*

1. High Magnetic Field Laboratory, Key Laboratory of High Magnetic Field and Ion Beam Physical Biology, Hefei Institutes of Physical Science, Chinese Academy of Sciences, Hefei 230031, Anhui, P. R. China.
2. University of Science and Technology of China, Hefei 230036, Anhui, P. R. China.
3. Institutes of Physical Science and Information Technology, Anhui University, Hefei 230601, Anhui, P. R. China.
4. School of Chemistry and Chemical Engineering, Hefei University of Technology, Hefei 230009, Anhui, P. R. China.

[#]These authors contributed equally: Kun Ma, Ze Wang, and Tongxiang Tao.

^{*}Corresponding authors: junfeng@hmfll.ac.cn (Junfeng Wang), qxl@ustc.edu.cn (Qingyou Lu), yanglu@hfut.edu.cn (Yang Lu)

1. Experimental equipment

7 T reaction furnace consists of a home-built furnace and a commercial superconducting magnet. In the furnace chamber (Figure 1A), a vacuum interlayer is used to insulate the heat conduction from the furnace heater. Liquid nitrogen flows outside the vacuum interlayer as the cooling medium. Another vacuum interlayer outside the liquid nitrogen insulates heat exchange between liquid nitrogen and helium, which is in the magnet Dewar to keep the coil at superconducting state. The photo of furnace chamber is shown in Figure S1.

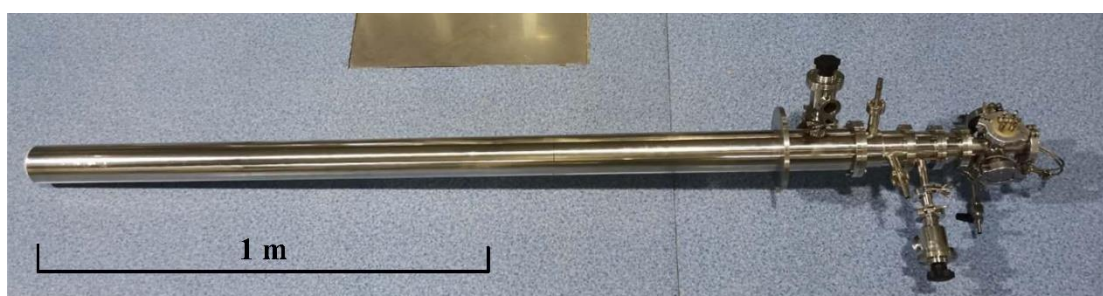


Figure S1. Photo of the furnace chamber.

2. Supplementary experimental details

Synthesis of MNPs

Typically, $\text{Fe}(\text{acac})_3$ (0.05 mmol) and 1,2-hexadecanediol (0.25 mmol) were mixed in 5 mL of diphenyl ether (containing 0.1% ultrapure water). Then 0.5 mmol of oleylamine and 0.5 mmol oleic acid were added to the reaction mixture in 60 °C water bath for 3 hours to make a homogeneous solution. The solution was transferred to a Teflon-lined stainless steel autoclave, and heated at 200 °C for 6 hours at different positions in 7 T reaction furnace. After cooling to room temperature, the synthesized nanoparticles were precipitated in ethanol and washed by ethanol for several times. The samples were stored in the chloroform for further experiments.

Characterization of MNPs

The self-assembly behavior of nanoreactor was analyzed by DLS at 25 °C on a Malvern Zetasizer Nano ZS (Malvern, UK). After 200 °C reaction, the solution was collected for DLS measurement. The MNPs were dispersed and dried on ultrathin carbon-coated

copper grids for TEM studies. Crystal size distribution of MNPs was analyzed by measuring both the length and width of at least 200 crystals in TEM images. The average of the long and short axis per crystal was taken as the crystal size. XRD data were recorded using a Philips X'Pert X-ray powder diffractometer. Magnetic properties were measured using a Quantum Design MPMS SQUID magnetometer (Model XP-5XL). For SQUID measurements, MNP samples were dried, loaded into gelatin capsules with wax, sealed, and fixed in a clear diamagnetic plastic straw. Magnetic hysteresis loops at 300 K were measured at ± 3 T.

MNPs ligand exchange

To render the MNPs hydrophilic, 20 mg DHCA and 6 mL tetrahydrofuran was added into a 25 mL flask. After that, the tetrahydrofuran with 10 mg MNPs was slowly added into the flask, and then heated, stirred and refluxed for 3 h. After cooling to room temperature, 0.5 mL 100 mM NaOH solution was added to precipitate MNPs. After centrifugation at 10000 rpm for 10 min, the MNPs were collected and resuspended in deionized water, stored at 4 °C.

***In vitro* MRI experiments**

The MR relaxation rate measurements were performed on a 3 T scanner (Achieva, Philips Medical systems, Best, The Netherlands) with a human head coil. The T_1 -weighted MR images were acquired using a turbo spin echo (TSE) sequence with the following parameters: TR/TE = 150, 300, 600, 1000, 2000, 4000, 8000/11 ms, slice thickness = 3 mm, a flip angle of 90°, the number of signal averages of 2, field of view (FOV) = 120 mm \times 120 mm, and matrix size = 240 \times 240.

***In vivo* MRI experiments**

In vivo MRI study of Fe₃O₄@DHCA MNPs was operated in healthy male mice (about 6-week-old) in which the average body weight is 20 grams. Animal experiments in this study were approved and carried out in accordance with the protocol provided by the Institutional Animal Care and Use Committee (IACUC) at Anhui Medical University. IACUC uses Guidelines for the ethical review of laboratory animal welfare, People's Republic of China National Standard GB/T 35892-2018 for the Care and Use of Laboratory Animals. The mice were anesthetized by intraperitoneal injection of 5%

chloral hydrate. Dosage of $\text{Fe}_3\text{O}_4@DHCA$ MNPs was 0.05 mmol Fe per kg mouse body weight in this study. The MR images were obtained with a 3 T scanner (Achieva, Philips Medical systems, Best, The Netherlands) equipped with a mouse coil. T_1 -Weighted images were acquired using a 3D fast field echo (FFE) sequence. FFE 3D sequence was used for MR imaging to scan the heart and vessels of mice.

3. Supplementary results

The water-cooled magnet mentioned above was used to control the synthesis of MNPs for the analysis the relation between mean size and field strength, excluding the influence of field gradient, because it can create highly homogeneous magnetic field. The mean sizes are 5.38, 5.25, 4.74, 4.61, 4.49, 4.31 nm when the intensity of treating fields are 1, 3, 5, 7, 9, 24 T respectively (Figure S3). The mean size decreases with the increase of field strength, which is similar to the results of 7 T reaction furnace.

The XRD results showed that the (311) peak becomes broader with the increase of treating magnetic field, meaning the mean size decreases, which agrees with the result of size distribution analysis. Meanwhile, the Raman spectrum confirms the $2A_{1g}$ with $3E_g$ and $5E_g$ peaks confirms the existence of magnetite at a high laser power of 24 mW. These features are characteristic of the iron oxide magnetite structure.

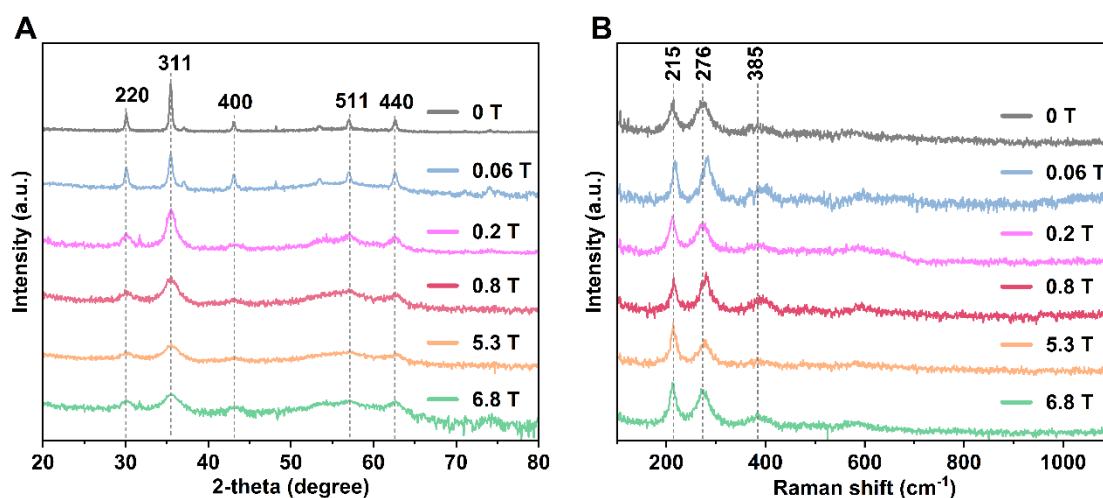


Figure S2. XRD results (a) and Raman spectra (b) of MNPs treated in different magnetic fields.

Reaction system in water-cooled magnet has a similar structure. One important difference is the cooling medium is water. Because the water-cooled magnet has a room temperature bore, the outer chamber is directly put into the magnet bore after cooled by the water (Figure S3).

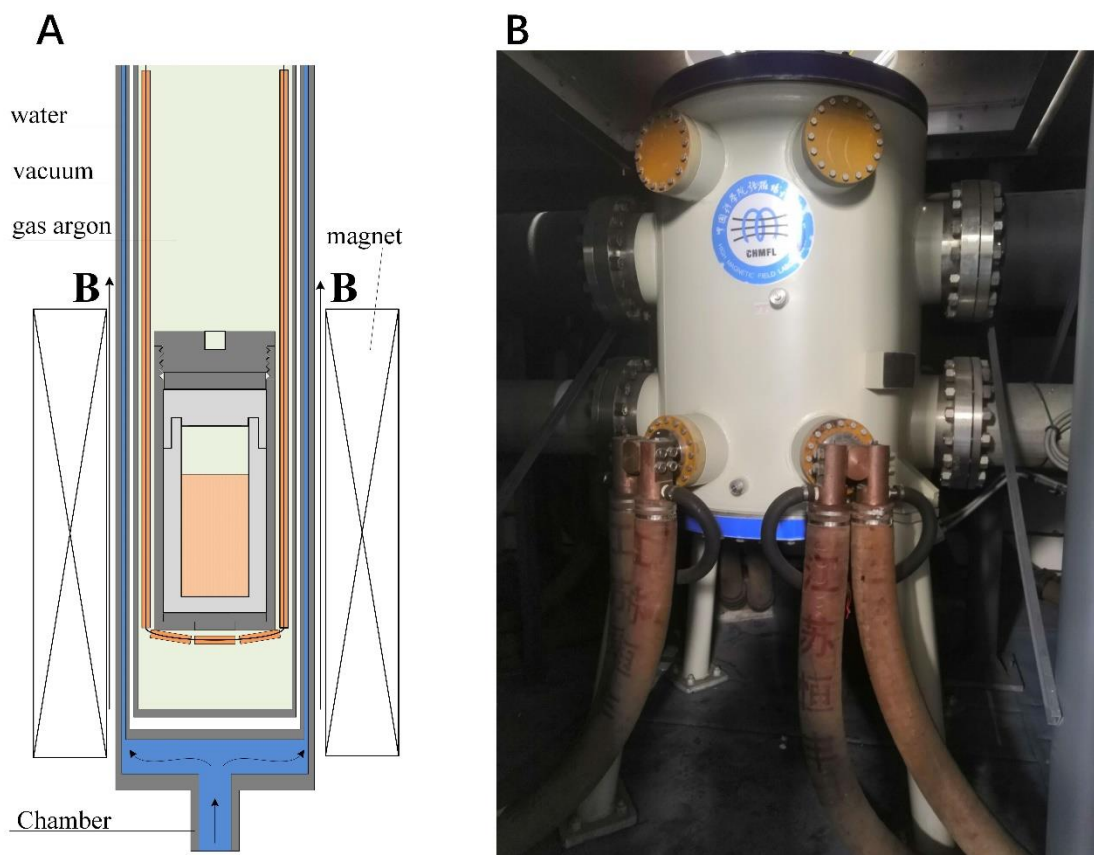


Figure S3. Reaction system in water-cooled magnet. (A) Sketch. (B) Photo of the 25 T water-cooled magnet.

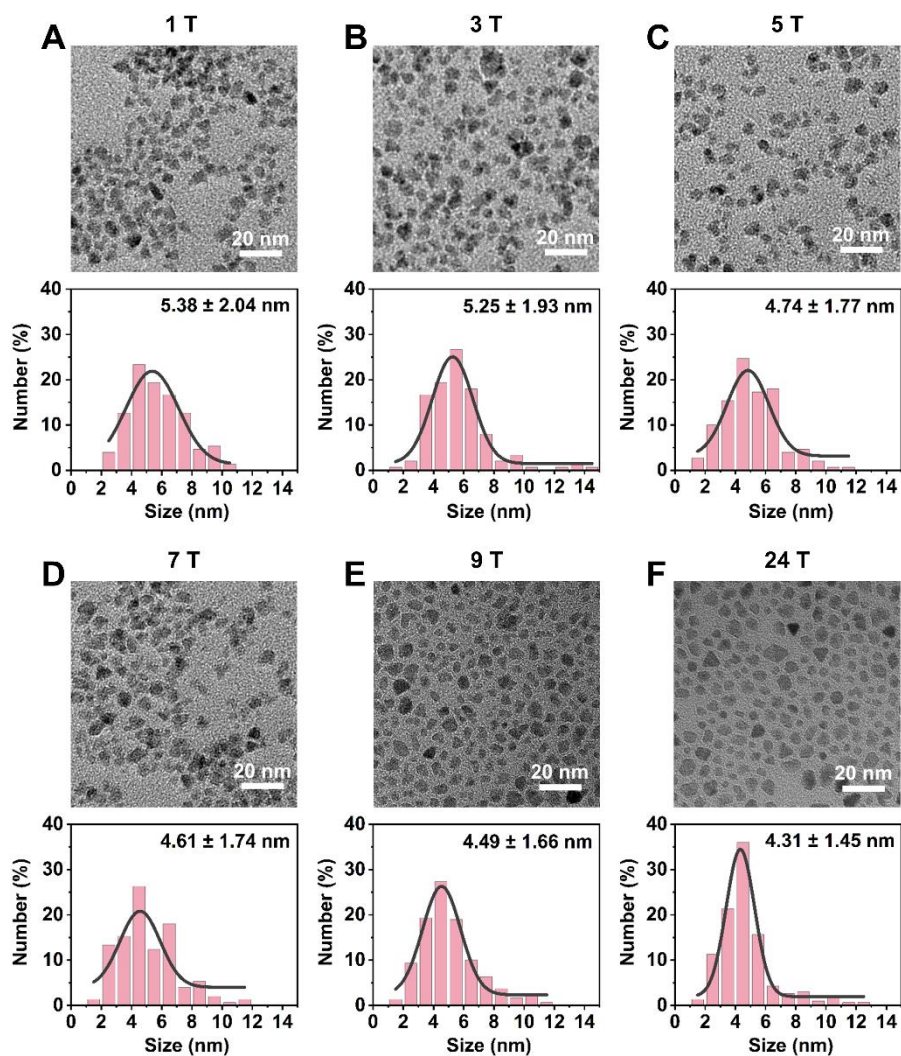


Figure S4. Morphology and size distribution of MNPs synthesized in different homogeneous magnetic fields (reaction system in a water-cooled magnet, Figure S3). The tops of (A)–(F) are TEM images, while the bottoms are statistical results for particle size.

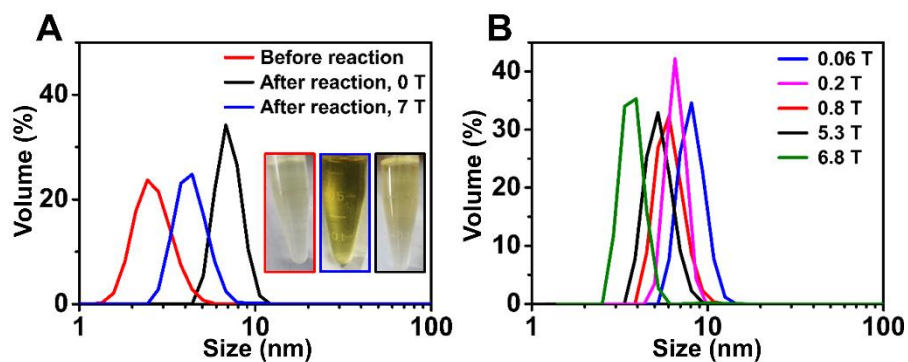


Figure S5. DLS measurement of solutions before and after reaction with 0 T (as control experiment) or different magnetic fields. (A) The 7 T results are from solution with its MNPs synthesized in homogeneous field. The photos with red, blue, black frame in insets are solutions related to the curves with the same color respectively. (B) The curves are measuring results of solutions after MNPs synthesis in gradient fields marked by different colors.

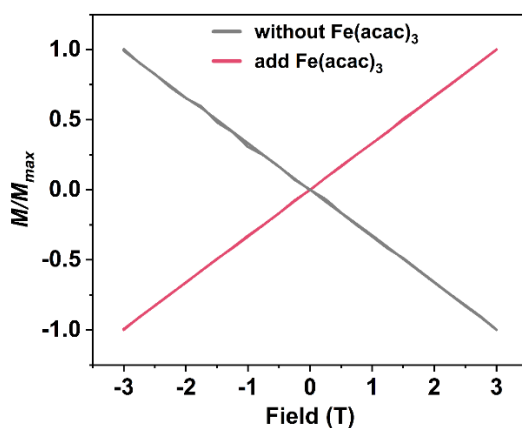


Figure S6. Field-dependent magnetization ($M-H$) curves of re-micelle without $\text{Fe}(\text{acac})_3$ and with $\text{Fe}(\text{acac})_3$ during synthesis.

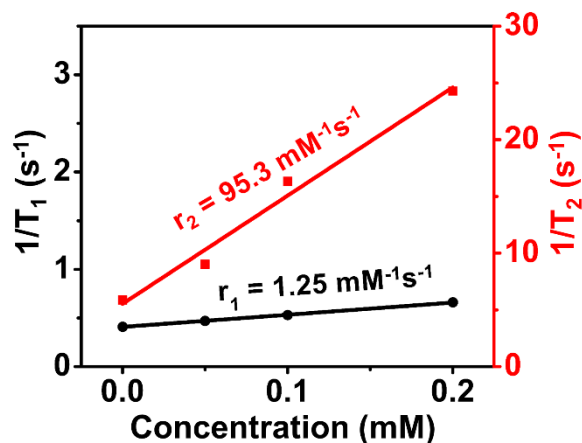


Figure S7. The r_1 and r_2 of $Fe_3O_4@DHCA$ MNPs in the control group on a 3 T MRI scanner (without magnetic field treatment)

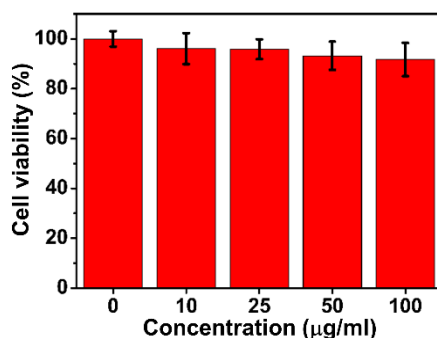


Figure S8. CCK-8 cell viability assay of HepG2 cells.

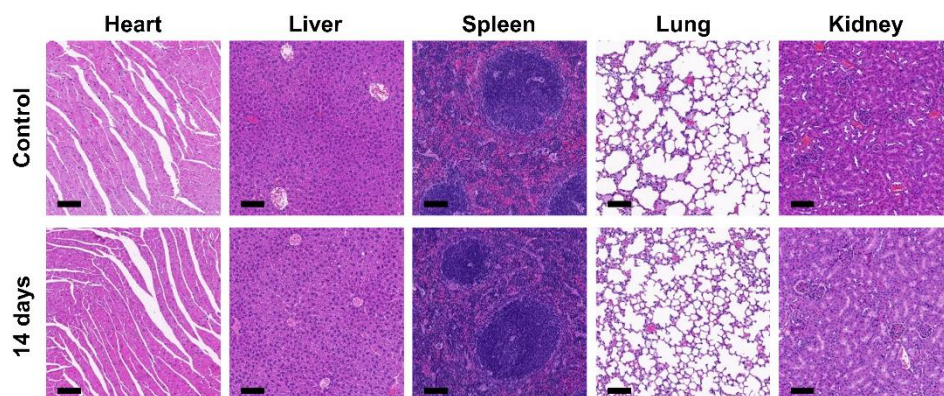


Figure S9. H&E-staining images of major organs of the mice. Representative images of organs harvested after 14 days' injection. The major organs did not exhibit any notable abnormalities. The scale bar is 100 μm . The control mice were injected by normal saline.

4. Discussion for dramatic drop in the curve

Use an exponential function to fit the red curve in Fig. 3 A, we can get the fitting formula 1 (FF1):

$$\bar{d} = a + b e^{-kB} = 4.4 + 6 e^{-5.8B}$$

In FF1, a is the diameter of the dotted circles in Fig. 4, $(a+b)$ is the re-micelle diameter when the treating field is zero, k is a constant. In FF1, we can define a constant treating field, B_0 , as:

$$\bar{d}_{B=B_0} = 0.5(a + b).$$

From the curve, B_0 is about 0.4 T. When the applied magnetic field is much larger than 0.4 T, the mean diameter does not change obviously with the increase of field strength. The effect is in saturation zone. When the field is not large enough, following discussion of chemical equilibrium change induced by magnetic field can explain the exponential decay relationship. Supposing the magnetic susceptibility of aggregate surfactant molecules is larger than free ones, write the system free energy as (J. Phys. Chem. 1975, 79, 2622–2626):

$$\Phi = N_S \mu_S + N_A \mu_A + \sum_{g=2}^{\infty} N_g (g \mu_B + \mu_g + g \kappa B^2) + kT (N_S \ln \frac{N_S}{F} + N_A \ln \frac{N_A}{F} + \sum_{g=2}^{\infty} N_g \ln \frac{N_g}{F})$$

where subscript S , A , g , is solution, free surfactant, aggregate surfactants respectively. And μ_B is size-independent part of standard chemical potential per molecule of aggregate surfactants. κ is magnetic potential coefficient, decided by magnetic susceptibility and size. **In this part, treat κ as constant for simple.** F is the total number of molecules:

$$F = N_S + N_A + \sum_{g=2}^{\infty} N_g .$$

Total number of surfactant molecule is constant:

$$N = N_A + g \sum_{g=2}^{\infty} N_g \equiv \text{Constant} .$$

Assuming the solution is dilute, we have:

$$\frac{\partial N_A}{\partial N_g} = -g, \frac{\partial N_S}{\partial N_g} = 0, \frac{\partial N_{g'}}{\partial N_g} = 0, \frac{\partial F}{\partial N_g} = 1 - g, \frac{1-g}{F} \approx 0, (1+g) \ll -g \ln \frac{N_A}{F}$$

At equilibrium state, the partial derivative of Φ with respect to N_g equals to 0. So,

$$-g\mu_A + g\mu_B + \mu_g + g\kappa B^2 + kT(-g \ln \frac{N_A}{F} + \ln \frac{N_g}{F}) = 0,$$

$$\frac{N_g}{F} = \left(\frac{N_A}{F}\right)^g \exp\left[-\frac{1}{kT}(\mu_B - \mu_A + \kappa B^2)g + \mu_g\right].$$

Let

$$\xi = \frac{N_A}{F} \exp\left[-\frac{1}{kT}(\mu_B - \mu_A + \kappa B^2)\right],$$

We can get:

$$\frac{N_g}{F} = \xi^g \exp\left(-\frac{\mu_g}{kT}\right).$$

Take the derivative with respect to g and let it be zero, we can get most possible g :

$$g_{mp} = \frac{\xi}{kT} \frac{d\mu_g}{dg} = g_{mp0} \exp\left(-\frac{\kappa B^2}{kT}\right).$$

Suppose g_{mp} is large enough to form a re-micelle. It is proportional to the surface area, so,

$$\bar{d} \propto \sqrt{g_{mp}} = \sqrt{g_{mp0}} \sqrt{\exp\left(-\frac{\kappa B^2}{kT}\right)} = \sqrt{g_{mp0}} \exp(-\alpha B), \alpha = \sqrt{\frac{\kappa}{kT}}.$$

From above formula, mean diameter decreases exponentially with the increase of magnetic field. Compared with FF1, a parameter is missing. This may because we used an overly simplified model.

5. Layer effect model

For simple, consider a system of two miscible liquids A, B. Liquids A and B have the same volume (V) and density, but different magnetic susceptibility. Let B has higher magnetic susceptibility for specification. The volume remains unchanged after mutual dissolution. Compare system energy before (state 1) and after (state 2) dissolution, we have:

$$\Delta U = U_2 - U_1 < 0$$

When a gradient magnetic field is applied, the field decreases from B_0 to 0 uniformly.

The system energy difference between state 1 and 2 turns to be:

$$\Delta U' = \Delta U + \Delta U_m = \Delta U + U_{m2} - U_{m1}.$$

Mark the total liquid height and cross section area as H , S , we have:

$$U_{m2} = \int_0^H \frac{1}{2\mu_0} (B_0 - \frac{z}{H} B_0)^2 \frac{\chi_A + \chi_B}{2} S dz = \frac{VB_0^2(\chi_A + \chi_B)}{6\mu_0},$$

$$U_{m1} = \int_0^{0.5H} \frac{1}{2\mu_0} (B_0 - \frac{z}{H} B_0)^2 \chi_A S dz + \int_{0.5H}^H \frac{1}{2\mu_0} (B_0 - \frac{z}{H} B_0)^2 \chi_B S dz = \frac{VB_0^2(7\chi_A + \chi_B)}{24\mu_0}.$$

So,

$$\Delta U' = \Delta U + \Delta U_m = \Delta U + \frac{VB_0^2(\chi_B - \chi_A)}{8\mu_0}.$$

From above, the total energy change can be positive when the magnetic field is strong enough. Positive energy change means state 1 is more stable, so the two liquids will be layered. However, when the susceptibility differential is small, the field is not strong enough to create a visible interface because of thermodynamic disturbance.